Annales Societatis Geologorum Poloniae (2013), vol. 83: 133–147.

MULTI-METHOD APPROACH TO VELOCITY DETERMINATION FROM ACOUSTIC WELL LOGGING

Jadwiga JARZYNA, Maria BAŁA & Paulina KRAKOWSKA

AGH University of Science and Technology, Faculty of Geology, Geophysics and Environment Protection, Department of Geophysics, Al. Mickiewicza 30, 30-059 Krakow, Poland, e-mails: jarzyna@agh.edu.pl, bala@geol.agh.edu.pl, krakow@agh.edu.pl

Jarzyna, J., Bała, M. & Krakowska, P., 2013. Multi-method approach to velocity determination from acoustic well logging. *Annales Societatis Geologorum Poloniae*, 83: 133–147.

Abstract: Three different methods of building detailed velocity models for seismic interpretation are explained and discussed in terms of their advantages and limitations. All of the proposed methods are based on the analysis of acoustic well logs. An application of acoustic full waveform measurements, as well as the FalaFWS and Estymacja software, is presented as a tool for determining P-wave and S-wave slowness (transit time interval, velocity reciprocal). Well log data from several wells, located near the special research seismic transect in the Polish Lowland, were processed using the methods proposed. The results of data analysis are presented for a depth section of up to 3623 m for the lithostratigraphic units, recorded from the Środa Wielkopolska 5 (SW5) well. The results of P-wave and S-wave slowness filtering, used to upscale well log data to a seismic scale of resolution, are shown for the entire geological profile of the SW5 well.

Key words: P-wave slowness, S-wave slowness, acoustic full waveforms, FalaFWS application, Estymacja program, acoustic wave frequency, seismic wave frequency.

Manuscript received 30 July 2012, accepted 7 October 2013

INTRODUCTION

Acoustic logging in wells is based on the same physical properties of rocks and the same elastic wave field as the seismic method, although there is a clear difference in the frequencies used in the two methods. Both approaches differ in vertical resolution, owing to the difference in frequency range: 15–20 kHz in a standard acoustic log and 6 kHz or lower in an acoustic full waveform, recorded with a dipole source, and 30–60 Hz in the seismic method (Boyer and Mari, 1997).

Within the frequency ranges mentioned above, the velocities of elastic waves, *i.e.* the compressional wave velocity, the shear wave velocity and the Stoneley wave velocity, do not show a clear dispersion. However, when a seismic velocity model appears unsatisfactory it is worth applying the correction, based on the quality factor (Q factor), which reduces the velocity of acoustic waves, compared to the velocity of seismic waves (Aki & Richards, 1980). This way, seismic records can be supplemented and improved by independently acquired information from acoustic well logging.

This paper explores and develops approaches and ideas preliminary presented in authors' previous work on seismic velocity calculations based on well log data (Jarzyna *et al.*, 2011b). Further studies on elastic waves velocity determination were carried out, using data from wells, located near the special research seismic survey line, selected for the project, "Improvement of the effectiveness of seismic survey for prospection and exploration for natural gas deposits in Rotliegend formations" (Górecki *et al.*, 2010). In the previous paper by the present authors, based on the results of this project (Jarzyna *et al.*, 2011b), emphasis was put on methodological aspects showing the difference in slowness values related to the results of measurements and processing. The outcomes were illustrated with examples from selected wells. In the present paper, authors focused on application of the methods proposed. Following a short description of the methodology, the results of three methods were presented. They were upscaled to seismic resolution to obtain velocity vs. depth curves and present the different vertical precision of the methods applied. The examples were chosen from well Środa Wielkopolska 5.

Acoustic full waveforms were the basis for S-wave velocity determinations, using the FalaFWS application in the GeoWin system (Jarzyna *et al.*, 2002, 2007). Regardless of the acoustic full waveforms, the velocity of an S-wave was calculated on the basis of theoretical formulas, using the Estymacja program (Bała and Cichy, 2003, 2006). The Estymacja software was used to calculate P-wave velocity, S-wave velocity and bulk density, using the results of the comprehensive interpretation of well logs (including determination of volume of selected rock-forming minerals and hydrocarbon saturation) and assuming theoretical values of selected elastic parameters.

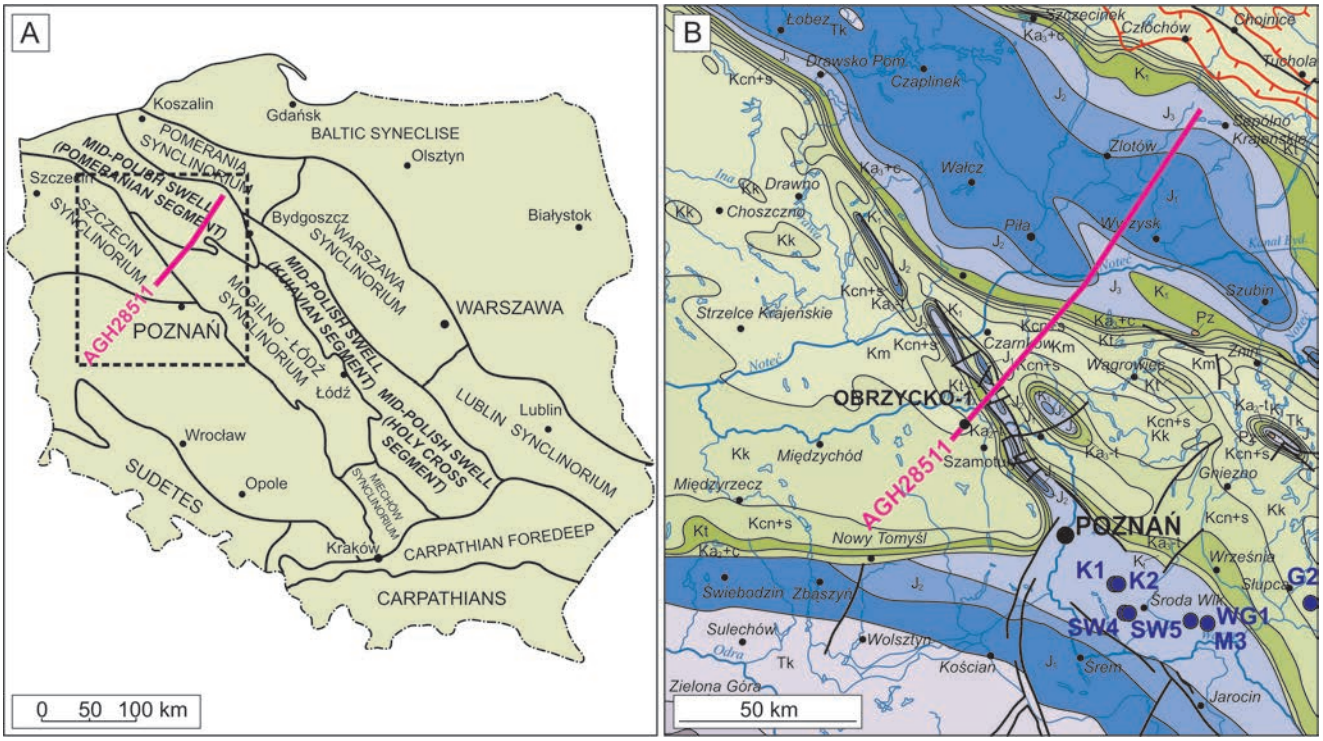

Fig. 1. General geology of study area. **A**. Location of study area and major structural units of Poland. **B.** Geology of study area below Cainozoic cover (Dadlez *et al.*, 2000). Location of study area shown as yellow rectangle and experimental regional seismic line used in structural interpretation as pink line. Green colours – Cretaceous, blue colours – Jurassic, pink colours – Triassic (after Dadlez *et al.* 2000; Pietsch *et al*. 2012)

P-wave and S-wave slowness derived from sonic logging with the FWS tool (Halliburton Logging Services) were available to the authors providing velocity of both types of elastic waves. However, in slow velocity formations, where the borehole-fluid velocity was higher than the formation S-wave velocity, the full slowness data range could not be recorded (Kimball and Marzetta, 1984). In these slow velocity depth intervals, the special processing of the acoustic waveforms was done using the FalaFWS application supplementing the missing data with correct results (V-Fala method) (Jarzyna *et al.*, 2010). In the logged depth sections, the porosity, mineral composition and hydrocarbon saturation of the formations were determined. These data were used in the Estymacja program to calculate the velocities of elastic waves, bulk density values and dynamic elastic moduli (V-EST method) (Bała and Cichy, 2003, 2006). In summary, there were values for P-wave velocity and S-wave velocity from three independent sources.

In order to scale the results of interpretation of well logs to the requirements of the seismic method, the processes of filtering and averaging, available in the FalaFWS application and the FunMat application from the GeoWin system, were used (Jarzyna *et al.*, 2007; Górecki *et al.*, 2010).

DATA SET AND GEOLOGICAL SETTING

Acoustic log data were used as a starting point for the construction of velocity models for seismic processing and interpretation, as well as for seismic modelling (Pietsch *et al.*, 2012; Marzec *et al.*, 2012). Wells with acoustic log data were selected near the seismic transect acquired for a research project, focused on the reservoir potential of sub-salt formations in the Polish Basin (Górecki *et al.*, 2010). The study area of the project was located in the Permo-Mesozoic sedimentary basin system of Western and Central Europe (Ziegler, 1990; Pharaoh *et al.*, 2010) (Fig. 1). The Mid-Polish Trough, which is part of this system, was initiated near the boundary of Carboniferous and Permian at the onset of the Rotliegend volcanism and sedimentation. The Permian and Mesozoic sediments, deposited in the study area, reach a total thickness of several kilometres. The seismic transect was located across a zone, characterized by Zechstein evaporites with a total thickness of approximately 1000–1300 m. The thick evaporite complex is covered by Mesozoic and Cainozoicsediments (Wagner, 1994). The criterion used in the selection of wells was the presence of the Rotliegend in the geological profiles penetrated by boreholes.

Acoustic full waveforms were available from several wells near the transect (WG1, SW4, SW5, M3, K1, K2 and G2; Fig. 1). The processing of acoustic data employed the same approach in all of the wells analysed. In this paper, the results obtained for the Środa Wielkopolska 5 (SW5) well are presented to illustrate the applicability of the methodology proposed. The geological profile in the SW5 well is representative for the study area. All geological units identified there (apart from the Cretaceous formation) are present in the geological profile of the SW5 well. The total thickness of the Rotliegend sediments in the SW5 well is greater than 100 m.

METHODOLOGY FOR DETERMINATION OF ELASTIC PROPERTIES

A short description of the proposed methods is presented to illustrate the differences in the approaches applied and their impact on the variability of the results.

Elastic parameters determined from acoustic full waveforms and FalaFWS computations

Acoustic full waveform measurements, as the direct result of logging by means of an FWS device, were the most important source of the P-wave slowness and S-wave slowness and Stoneley wave slowness (Kimball and Marzetta, 1984). The measurements provided good results for P-wave slowness (DTP) in the majority of cases, but reliable data on S-wave slowness (DTS) were available only in the depth sections, where the shear wave velocity (V_S) was higher than the velocity in mud (V_M). If this was not the case, blind sections appeared in the S-wave velocity profiles (Fig. 2). Such blind sections were visible at depths between 1780–2010 m, 2260–2300 m, 2980–3000 m. The primary acoustic logging results, i.e. DTP and DTS from the FWS device recording are treated as the first method (V-FWS) of slowness determination.

In the depth intervals where $V_M > V_S$, the modified FalaFWS application of the GeoWin computer system was used to determine S-wave velocity (Jarzyna *et al.*, 2010). P-wave velocity and Stoneley wave velocity were also determined, using an improved FalaFWS application to confirm the good quality of FWS device recordings. The slowness or velocity of acoustic waves, determined from the processing and interpretation of acoustic full waveforms with the use of FalaFWS application, is the second method (V-Fala) of slowness determination.

The comparison of P-wave slowness from V-FWS method and from V-Fala method showed very good agreement of these results (Fig. 3). A high value of the determination coefficient for the relationship between DTP FWS and DTP Fala demonstrated the similarity of these results. S-wave slowness revealed a slightly worse correlation, but the results were also satisfactory (Fig. 3). In both cases, the dispersion of data was observed. A higher dispersion in the case of S-waves resulted from the greater scatter of S-wave slowness (DTS) values, obtained from S-wave processing, although values of the semblance function in the S-wave packet were quite high (Fig. 4). The raw data were recorded at depth intervals of 0.1 m and the primary processing of raw data was also done with the same depth interval. Next, the results were smoothed and the dispersion was reduced. Examples of outcomes of the FalaFWS computer program for the SW5 well in two depth sections with diverse lithologies are presented in Figures 4 and 5. Figure 4 shows the results for the V-Fala method in the SW5 well, in a section of the Upper Muschelkalk (limestones, marlstones). A set of outcomes from FalaFWS without averaging, as a result of data recording and processing at each 0.1 m interval, is presented in the left hand side track. In the middle track, the slowness of P-wave, S-wave and Stoneley wave after use of an 11-point moving average are shown together with velocity ratio, VP/VS and Poisson ratio and values of semblance function. In the right-hand track, the same results after 25-point averaging are shown. Similar results are presented (Fig. 5) for the V-Fala method, applied to the Lower Triassic (Lower Bunter Sandstone) formation (calcareous claystones, mudstones, sandstones) in the SW5 well. This example illustrates the influence of lithology on slowness and shows that the processing of acoustic full waveform data at each measured point yields results that are too detailed. The averaging calculation, using 11 and 25 points for distances of 1 m and 2.5 m, respectively, produced smoothed curves that were much more definitive, but still not upscaled to the seismic scale.

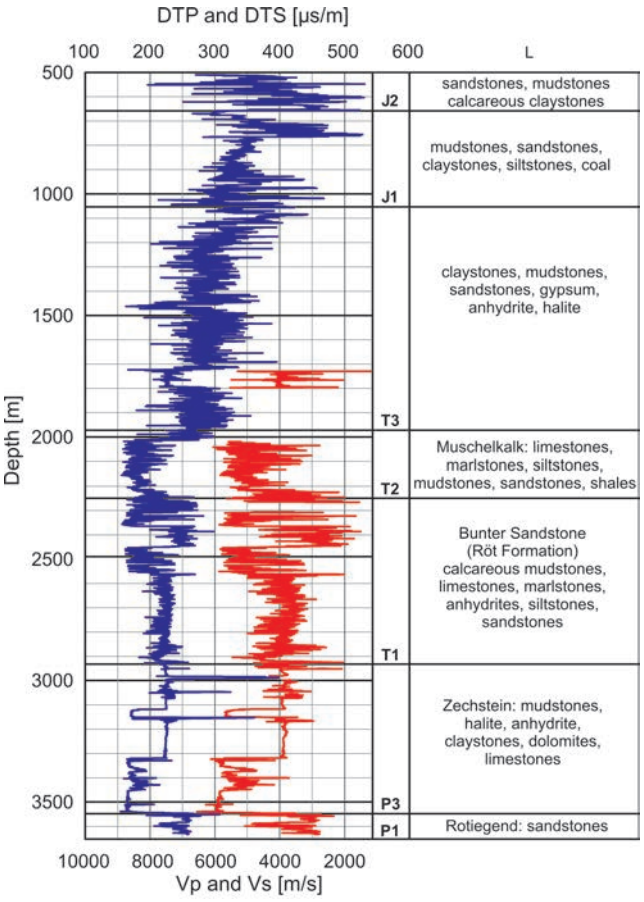

Fig. 2. Results of V-FWS method in SW5 well; lack of DTS in some intervals, where V_P of mud is higher than V_S of formation. Symbols: L – lithology, J2 – Middle Jurassic, J1 – Lower Jurassic, T3 – Upper Triassic, T2 – Middle Triassic, T1 – Lower Triassic, P3 – Upper Permian, P1 – Lower Permian, DTS – S-wave slowness, V_P – P-wave velocity, V_S – S-wave velocity

Automatic interpretation of acoustic full waveforms, using the FalaFWS application, was the basis for slowness determinations. This was done with a vertical sampling interval of 0.1 m in all depth sections of the well, where full waveform acoustic data were available (Fig. 3). The results of this interpretation were used for the calculation of basic statistical values of the elastic parameters and for the averaging of data to permit upscaling. Calculations of compressional wave slowness, shear wave slowness and Stoneley

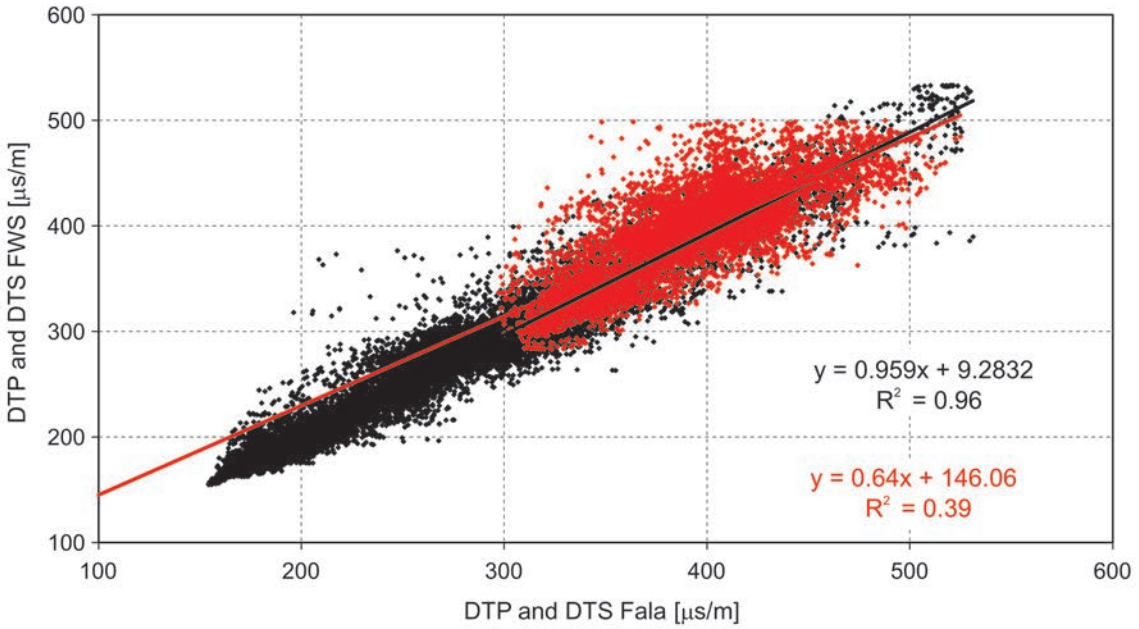

Fig. 3. Comparison of DTP (black) and DTS (red) results from V-FWS method in SW5 well (DTP and DTS FWS) and from V-Fala method (DTP and DTS Fala after processing with FalaFWS application)

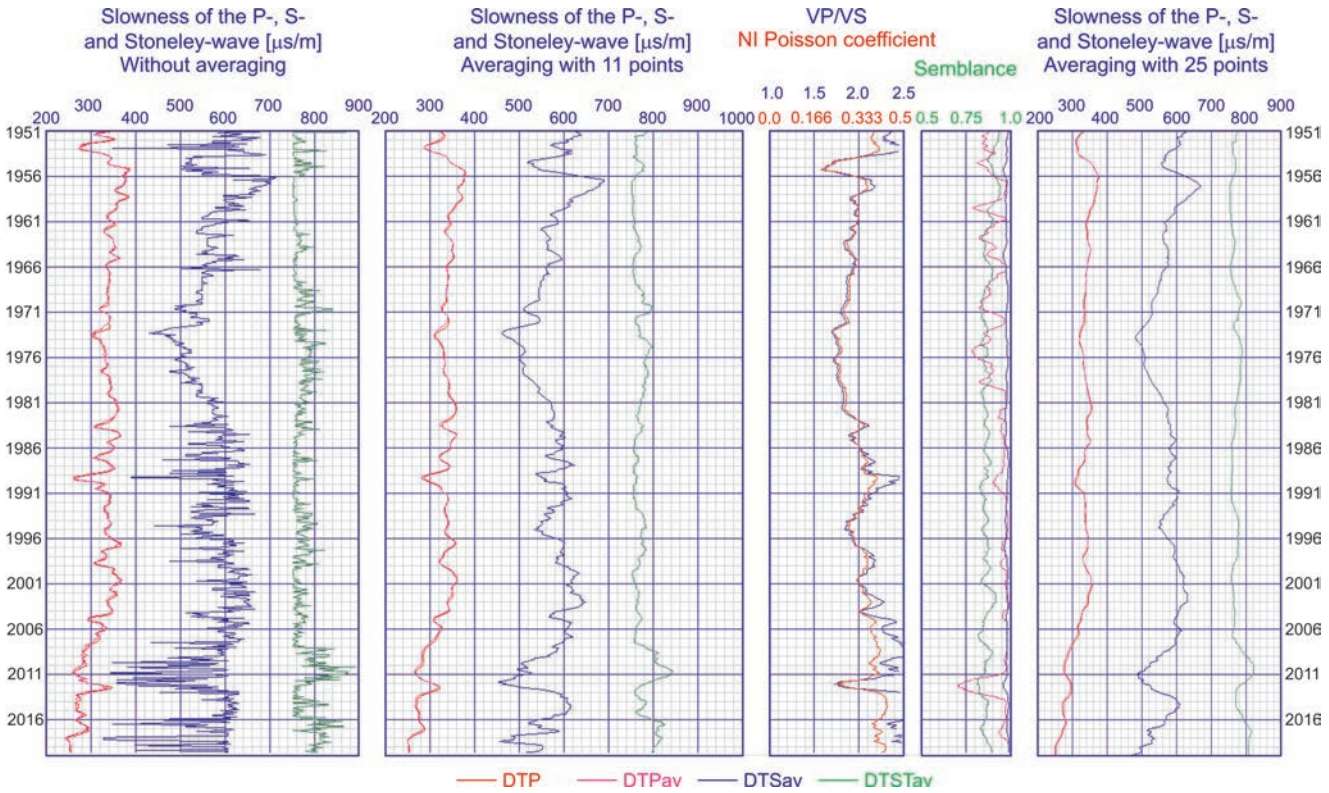

Fig. 4. Results of V-Fala method in SW5 well, Upper Muschelkalk (limestones, marlstones); set of outcomes from FalaFWS application without averaging, data recorded and processed at each 0.1 m (left-hand side), after 11 points averaging (middle part), after 25 points averaging (right-hand side)

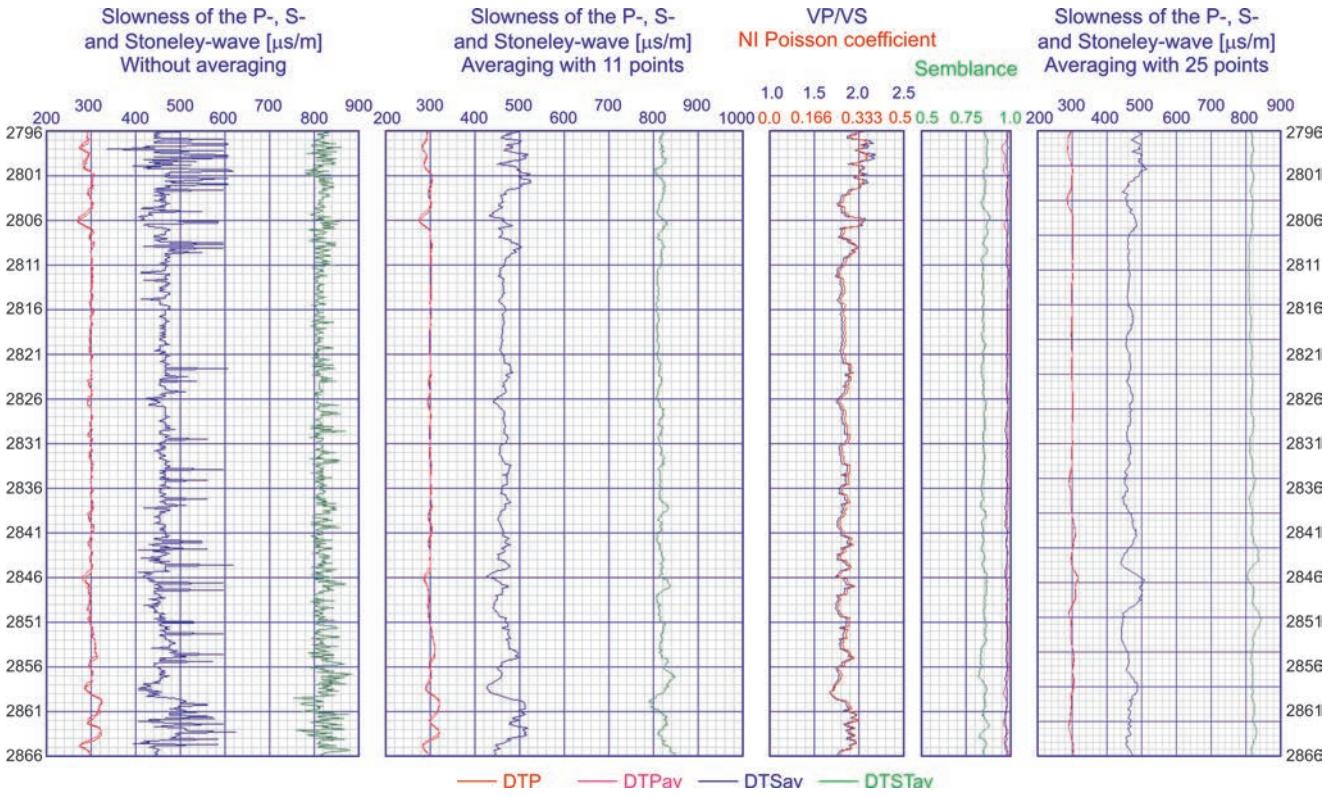

Fig. 5. Results of V-Fala method in SW5 well, Lower Triassic (Lower Bunter Sandstone) formation (calcareous claystones, mudstones, sandstones); set of outcomes from FalaFWS application without averaging, data recorded and processed at each 0.1 m (left-hand side), after 11 points averaging (middle part), after 25 points averaging (right-hand side)

wave slowness were done in FalaFWS, utilising the semblance algorithm for six pairs of acoustic waveforms (Kimball and Marzetta, 1984).

Elastic parameters determined from Estymacja program

The third data set, comprising P-wave velocity, S-wave velocity and Stoneley wave velocity and also bulk density, was obtained from the Estymacja program (Bała and Cichy, 2007). Estymacja utilises the theoretical Biot-Gassmann model to describe porous media (Biot, 1956; Gassmann, 1951). Values of compressional wave velocity (VPEQ) and slowness (DPEQ) and shear wave velocity (VSEQ) and slowness (DSEQ), elastic moduli (EEQ, KEQ, MIEQ), the VPEQ/VSEQ ratio and Poisson's ratio (NIEQ), as well as bulk density (RHEQ) were determined from Estymacja (V-EST method). The results of the comprehensive interpretation of well logs were used as input data for the computer program (Górecki *et al.*, 2010), with regard to the volumes of individual mineral components of the matrix, porosity and water saturation. The admixture of accessory minerals was determined through laboratory investigations, i.e., Scanning Electron Microscopy (SEM), or X-ray Diffraction (XRD). The matrix parameters included: Kma – bulk modulus of matrix, MIma – shear modulus of matrix, ρma – bulk density of matrix, DTma – matrix slowness and bulk moduli of pore water, gas or oil. The matrix parameters were assigned, according to the mineral composition of each stratigraphic unit. The parameters of minerals and bulk moduli of porous media were available in the public domain (Bała, 1994; Halliburton Logging Services, 1991). The Estymacja program generated theoretical logs, which were compared with the recorded acoustic log and the bulk density log. This comparison was done to accurately define the matrix parameters for each of the mineral components, thus minimizing the error of estimation (δ). The error was calculated, according to the formula (1):

$$\delta = [(DPEQ - DT(PA))/DT(PA)] \times 100\% \quad (1)$$

where: DPEQ – P-wave slowness from the V-EST method, DT(PA) – P-wave slowness from standard acoustic measurements.

Errors were calculated at each depth and presented as one of the resulting curves of the Estymacja program (error track in Fig. 6). The plots of calculated (red) and recorded data (black) in the Rotliegend sandstone formations in the SW5 well were presented as the results of the V-EST method (Fig. 6). The property ranges are indicated below the header of each column. The Rotliegend formation, comprising brown and red fine-grained and middle-grained sandstones, was analysed at depths between 3545 and 3648 m. The following specific parameters were set for the sandstone component: ρma = 2.65 g/cm^3, Kma = 27 GPa, MIma = 28 GPa, for clay component: ρma = 2.65 g/cm^3, Kma = 16.829 GPa, MIma = 7.036 GPa, for gas: ρ_g = 0.1 g/cm^3, Kg = 0.05 GPa, for water: ρw = 1.03 g/cm^3, Kw = 2.638 GPa. The selected unit was associated with significant porosity and water saturation.

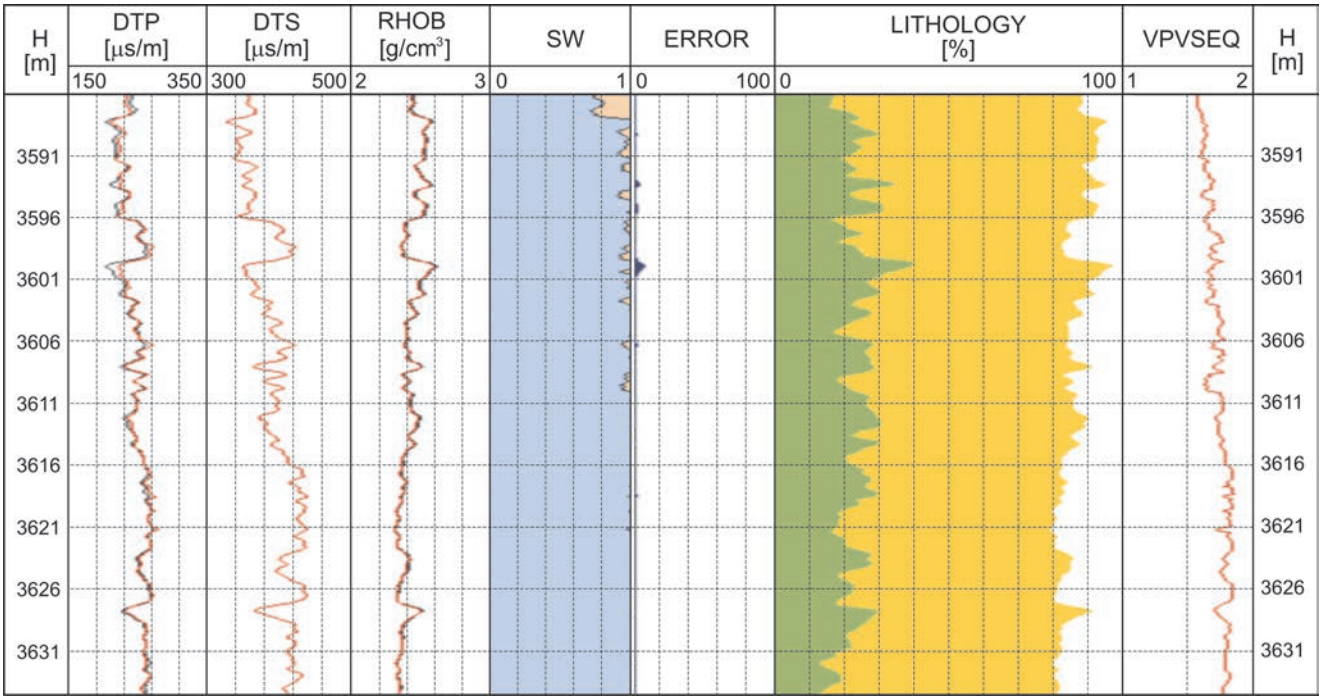

Fig. 6. Parameters calculated in Estymacja program expressed as red lines; logs recorded in Rotliegend formation in SW5 well at depths 3586–3648 m shown as black lines; proportions of sandstone, shale and porosity are represented by yellow, green and white colours, respectively; gas saturation (1-SW) and water saturation (SW) are shown in rose and blue, respectively; curves are as follows: compressional wave slowness (DTP), shear wave slowness (DTS), bulk density (RHOB), water saturation (SW), estimation error (d), velocity ratio (VPVSEQ)

Histograms of the VPEQ and VSEQ values as well as the VPEQ/VSEQ ratio for the Rotliegend formation are shown in Figure 7. All histograms revealed the majority of data in the first class. This means that low values of VPEQ and VSEQ and RHEQ dominated as results of V-EST method. The majority of VP/VS data also belonged to the first class, although it was observed that the second small maximum in the class focused around VP/VS = 1.61. The first group of VP/VS data (around VP/VS = 1.57) was associated with strata that have a relatively high gas saturation, while the second group was associated with water saturated sandstones. Similar distributions of results, obtained from the V-EST method, were observed in other wells (Jarzyna *et al.*, 2011a).

A comparison between the results of the V-EST method and the V-Fala method was done on the basis of the data set, related to the P1 unit (Rotliegend sandstone). The basic statistics (average, minimum, maximum, standard deviation values) of parameters from the V-EST method are presented in Table 1. They are supplemented by average values of the V-FWS method (DTP FWS, DTS FWS) and RHOB measurement and also results from the V-Fala method (DTP Fala, DTP Fala) to make the comparison and identify properties of the Rotliegend sandstone.

Each of the methods, used to determine interval transit time (slowness) of P-waves and S-waves, had their advantages and limitations. The V-FWS method provided the slowness values (DTP and DTS) immediately after the borehole measurements. However, there were a number of depth intervals, where records of S-wave slowness could

Table 1

Basic statistics of Rotliegend sandstones in SW5 well at depths of 3545–3648 m

P1 - Rotliegend sandstone	Average	Minimum	Maximum	Standard deviation
DPEQ [µs/m]	262	210	352	20
DSEQ [µs/m]	410	322	543	32
EEQ [GPa]	33.44	15.88	57.73	6.60
KEQ [GPa]	16.24	7.28	25.83	3.19
MIEQ [GPa]	14.47	6.99	25.60	2.90
NIEQ	0.16	0.12	0.20	0.02
RHEQ [g/cm^3]	2.38	2.06	2.65	0.09
VPEQ [km/s]	3.84	2.84	4.76	0.30
VSEQ [km/s]	2.45	1.84	3.11	0.20
VPVS	1.57	1.52	1.63	0.03
DTP FWS	245	155	308	20
DTS FWS	421	272	484	40
RHOB	2.41	2.21	2.80	0.08
DTP Fala	244	156	294	20
DTS Fala	583	330	709	82

DPEQ, DSEQ, EEQ, KEQ, MIEQ, NIEQ, RHEQ, VPEQ, VSEQ, VPVS – P-wave slowness, S-wave slowness, Young modulus, bulk modulus, shear modulus, Poisson ratio, bulk density, P-wave velocity, S-wave velocity, P-wave and S-wave velocity ratio, respectively (from V-EST method), DTP FWS, DTS FWS, RHOB- P-wave slowness, S-wave slowness, bulk density, respectively (from V-FWS method), DTP Fala, DTS Fala- P-wave slowness, S-wave slowness, respectively (from V-Fala method)

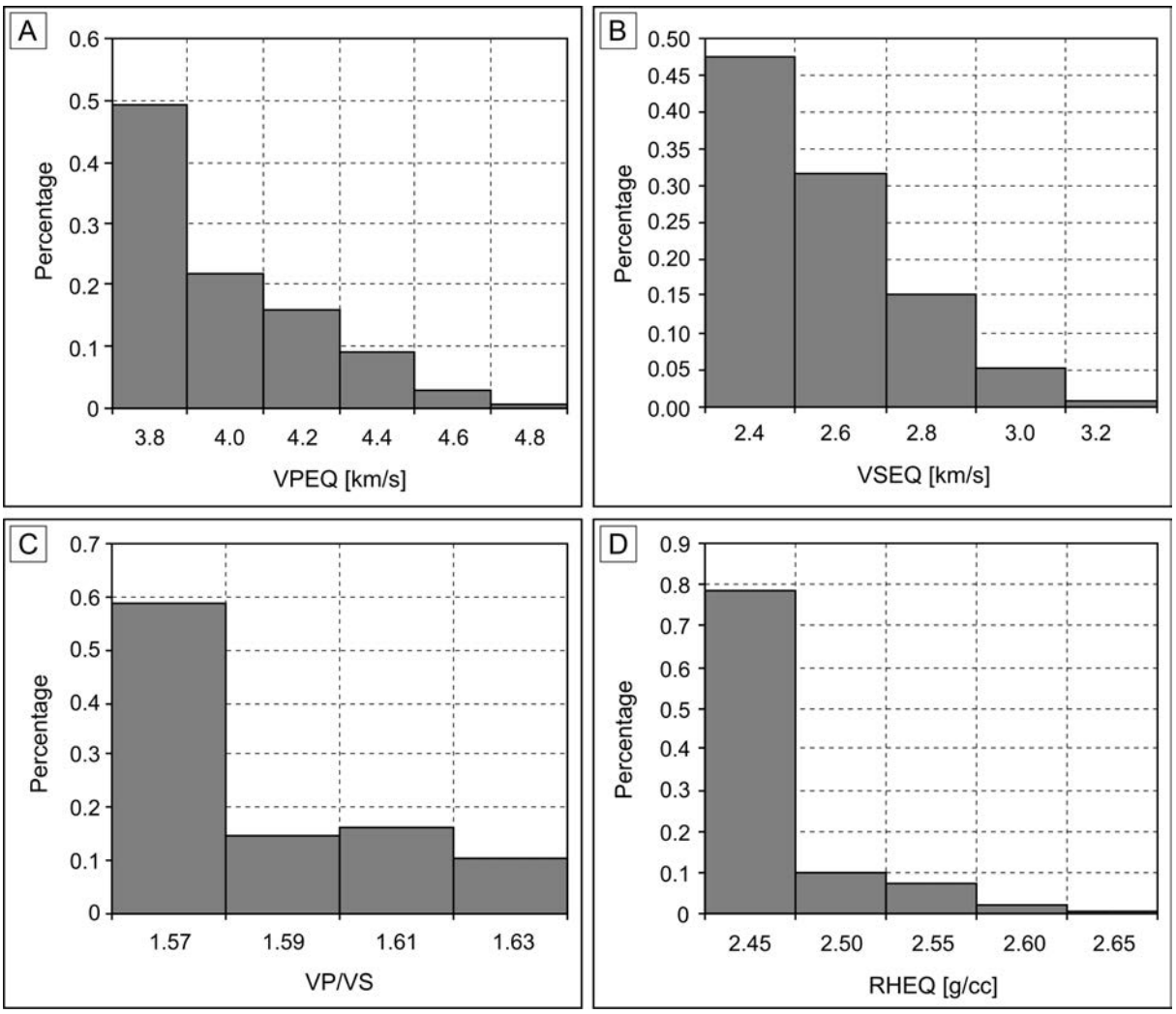

Fig. 7. Histograms of outcomes from V-EST method in SW5 well for Rotliegend formation a) velocity of P-wave (VPEQ); b) velocity of S-wave (VSEQ); c) velocity ratio (VPVS); d) bulk density (RHOB)

not be directly obtained. These depth intervals were associated with rock formations with poor elastic properties, fractured, and with high clay content. In such depth sections, the missing results were supplemented with data interpreted by the V-Fala method. Both methods yielded results only in the intervals, where the full waveform data was recorded.

The V-EST method provided slowness values from all depth intervals, where the comprehensive interpretation for lithology, porosity and water saturation was done. Most often, these sections of wells were longer than those where the available data had been recorded directly with the FWS tool. The first two methods provided slowness data measured *in situ*. Thus, they were influenced by the recording conditions, such as variable well diameter, changes in borehole fluid parameters with depth, and a distorted configuration of the sonic tool in the well. In order to perform calculations in the V-EST method, it was necessary to set the elastic parameters of matrix components and the parameters related to the pore fluids. The accuracy of the adopted lithological composition and the matrix parameters determined the accuracy of the V-EST method results. The results of interpretations in the V-Fala method depended also on the vertical distance between recording points and the vertical sampling interval, adopted for the interpretation. Similarly, the vertical sampling interval, adopted for the calculations performed in the V-EST method, affected the results. The results were averaged at each stage of data processing and interpretation.

The consistency of the P-wave slowness values, determined from the V-FWS method (DTP FWS), and the V-EST method (DPEQ), is high. The coefficient of determination of 0.9 indicated that both sets of values could be used. A similar statement was true for S-wave slowness (Fig. 8), although here the determination coefficient is not as high. The dispersion of results around the correlation line is not significant. Several outliers can be adjusted during the analysis of the results from each stratigraphic unit. However, there was a clear concentration of results around the correlation line. The results for the V-FWS method (DTS FWS) were lower than those calculated in the V-EST method (DSEQ). The plots in Figure 8 were prepared, using data averaged with a vertical sampling interval of 2.5 m.

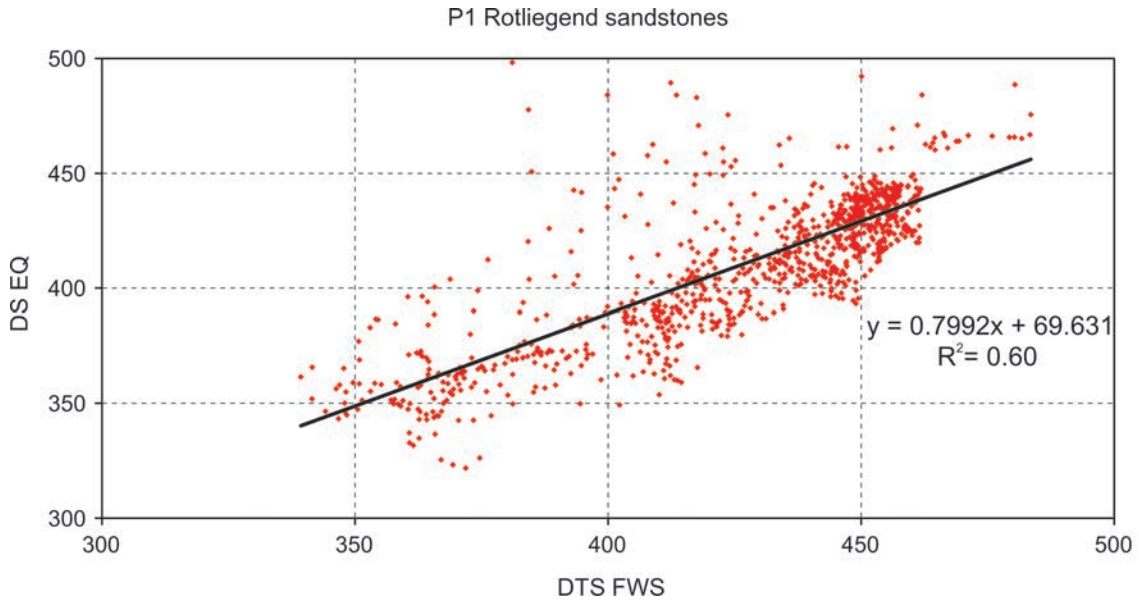

Fig. 8. Comparison of S-wave slowness V-FWS method (DTS FWS) with data calculated by V-EST method (DSEQ) in SW5 well for depths 3545–3648 m

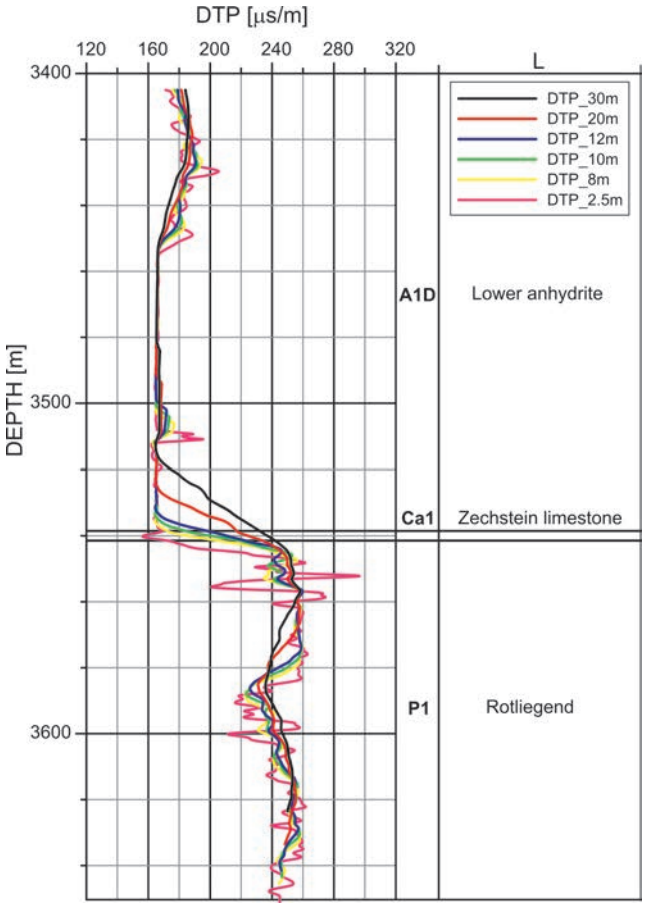

Fig. 9. Results of averaging of data using FalaFWS software in SW5 well for section comprising part of Upper Permian, Zechstein, Lower Anhydrite (A1D), Zechstein Limestone (Ca1) and Rotliegend formation (P1). Symbols: DTP_P – wave slowness, L – lithology, DTP_30m – DTP after 30 m averaging, DTP_ 20m – DTP after 20 m averaging, DTP_12m – DTP after 12 m averaging, DTP_10m – DTP after 10 m averaging, DTP_ 8m – DTP after 8 m averaging, DTP_ 2.5m – DTP after 2.5 m averaging

Filtration of P-wave slowness and S-wave slowness to construct velocity model for seismic interpretation

The results of the V-Fala method were the basis for averaging the slowness of P-waves and S-waves to prepare a suitable velocity model for seismic interpretation. Data from the SW5 well, grouped for individual stratigraphic units, were used for tests.

The primary data from the FWS measurements were presented with 0.1 m depth interval. Such results generated a data set of high precision, but too complex for the construction of a velocity model. Oversampling may cause a problem of redundancy and accuracy of results (Theys, 1999). Therefore, averaging was done for a depth window of 8 m and for depth windows of 10 m, 12 m, 20 m and 30 m. The basis for the averaging was a data set, sampled at intervals of 2.5 m. Calculations were performed for all data, using the V-Fala method (Table 2). Here, a running average was adopted as a filter for detailed events noted in the logs, which were related to geological layers of thickness, considerably below the seismic scale of resolution. Table 2 juxtaposes the values of P-wave slowness and S-wave slowness that were obtained by the different methods. The two main parts of the table show the results of FWS measurements and averaged results, derived from the V-Fala method. Table 2 includes statistics for the intensity of the natural radioactivity measured in well logs (GR) and bulk density (RHOB) to show the impact of lithology on the results obtained. The standard deviation (S.D.) was presented to show the diversity in values of the parameters. A mean value of filtering results (M) was included in the last column of Table 2. The values from Table 2 do not show any important difference between the means, calculated for depth windows from 2.50 m to 30 m (Figs 9, 10).

In the lower part of SW5 well profile (low rows in Table 2), several DTS values were removed after filtering, because a DTS exceeding 500 µs/m was inacceptable for

Table 2

Results of P-wave slowness and S-wave slowness filtering derived from FalaFWS for chronostratigraphic units in SW5 well

Log unit	Results of V-FWS method				Results of V-Fala method						
					Averaging in depth section of meters:						
	Av	Min	Max	S.D.	30	20	12	10	8	2.5	M
Upper Jurassic, J3 (355-544.9 m), N = 1900											
RHOB [g/ccm]	2.39	2.1	2.59	0.08							
GR [API]	32	11	67	10							
DTP [µs/m]	345	235	449	43	344	343	342	342	342	342	343
DTS [µs/m]					497	494	489	484	479	464	485
Middle Jurassic, J2 (545-655.9 m), N = 1110											
RHOB	2.21	1.97	2.77	0.09							
GR	68	23	110	15							
DTP [µs/m]	413	196	531	54	406	409	412	413	423	414	413
DTS [µs/m]					523	514	515	511	505	468	506
Lower Jurassic, J1 (656-1035.9 m), N = 3800											
RHOB	2.27	1.81	2.82	0.1							
GR	47	11	114	29							
DTP [µs/m]	346	213	528	44	346	346	345	345	345	345	345
DTS [µs/m]					513	509	496	488	482	442	488
Upper Triassic, Rhaetian Tre (1036-1441.9 m), N = 4060											
RHOB	2.39	1.75	2.77	0.15							
GR	70	30	128	11							
DTP [µs/m]	308	201	443	40	304	305	306	306	307	307	306
DTS [µs/m]					460	452	446	441	432	396	438
Upper Triassic, Upper Keuper Tk3G, Upper Gypsum Series (1442-1633.9), N = 1920											
RHOB	2.41	1.63	2.98	0.24							
GR	75	8	96	15							
DTP [µs/m]	283	163	387	34	284	282	282	282	282	281	282
DTS [µs/m]					488	471	429	417	402	358	428
Upper Triassic, Upper Keuper Tk3T, Stuttgart Formation/Schilfsandstein (Reed Sandstone) (1634-1709.9 m), N = 760											
RHOB	2.39	1.71	2.63	0.14							
GR	54	9	124	29							
DTP [µs/m]	281	233	395	20	276	278	279	279	279	279	278
DTS [µs/m]					386	384	383	382	381	369	381
Upper Triassic, Upper Keuper Tk3D, Lower Gypsum Beds (1719-1897.7 m), N = 1880											
RHOB	2.44	1.86	2.94	0.26							
GR	52	9	106	27							
DTP [µs/m]	256	166	341	29	255	254	253	253	253	253	253
DTS [µs/m]	407	323	541	21	386	384	383	382	381	369	381
Upper Triassic, Lower Keuper Tk1 (1898-1988.9 m), N = 910											
RHOB	2.5	2.11	2.72	0.1							
GR	73	23	106	17							
DTP [µs/m]	276	195	355	23	270	272	272	272	273	274	272
DTS [µs/m]					482	477	459	453	447	425	457
Middle Triassic, Upper Muschelkalk Tm3 (1989-2029.9 m), N = 410											
RHOB	2.66	2.52	2.76	0.06							
GR	49	15	77	15							
DTP [µs/m]	223	159	298	41	198	205	213	215	216	221	211
DTS [µs/m]	340	321	385	17	364	341	324	321	321	313	331

Table 2 continued

Log unit	Results of V-FWS method				Results of V-Fala method						
					Averaging in depth section of meters:						
	Av	Min	Max	S.D.	30	20	12	10	8	2.5	M
Middle Triassic, Middle Muschelkalk Tm2 (2030-2078.9 m), N = 490											
RHOB	2.78	2.58	2.95	0.09							
GR	37	12	64	12							
DTP [μs/m]	188	158	239	20	187	187	187	187	188	187	187
DTS [μs/m]	362	297	461	36	354	341	322	320	318	300	326
Middle Triassic, Lower Muschelkalk Tm1 (2079-2256.4 m), N = 1775											
RHOB	2.68	2.32	2.76	0.06							
GR	33	15	61	11							
DTP [μs/m]	187	156	268	15	188	187	186	186	186	185	186
DTS [μs/m]	365	308	501	33	323	318	316	315	313	300	314
Lower Triassic, Upper Bunter Sandstone (Röt Formation) Tp3 (2256.5-2365.4 m), N = 1090											
RHOB	2.75	2.56	2.94	0.1							
GR	47	15	101	19							
DTP [μs/m]	202	157	282	32	202	201	200	200	200	199	200
DTS [μs/m]	366	307	523	50	323	314	310	308	305	299	310
Lower Triassic, Middle Bunter Sandstone Tp2 (2365.5-2579.9 m), N = 2145											
RHOB	2.64	2.16	2.76	0.07							
GR	79	17	151	40							
DTP [μs/m]	218	162	299	30	216	216	217	217	217	218	217
DTS [μs/m]	399	307	525	55	321	315	307	300	293	283	303
Lower Triassic, Lower Bunter Sandstone Tp1 (2580-2918.9 m), N = 3390											
RHOB	2.69	2.64	2.75	0.02							
GR	92	59	117	8							
DTP [μs/m]	222	183	250	9	222	222	221	221	221	221	221
DTS [μs/m]	405	327	471	20	368	359	351	349	346	331	351
Upper Permian, Transition Mudstones IP (2919-2932.9 m), N = 140											
RHOB	2.58	2.35	2.80	0.11							
GR	77	37	98	19							
DTP [μs/m]	234	192	259	14	224	225	228	229	231	233	228
DTS [μs/m]	433	360	498	33	401	387	381	381	382	381	386
Upper Permian, Zechstein, Youngest Halite Na4 (2933-2981.9 m), N = 490											
RHOB	2.05	1.83	2.34	0.04							
GR	6	3	36	3							
DTP [μs/m]	224	215	260	4	244	240	231	228	226	223	232
DTS [μs/m]	408	362	496	19	400	387	381	381	381	381	385
Upper Permian, Zechstein, Pegmatite Anhydrite A4D (2982-2983.1 m), N = 12											
RHOB	2.33	2.06	2.5	0.18							
GR	9	5	25	6							
DTP	217	210	224	5	275	301	345	338	321	224	301
DTS					458	476	485	471	452	402	457
Upper Permian, Zechstein, Red Clay I4 (2983.2-2993.4 m), N = 103											
RHOB	2.21	2.08	2.48	0.06							
GR	55	19	68	12							
DTP [μs/m]	353	228	399	41	254	268	301	315	328	348	302
DTS [μs/m]					442	435	457	463	451	405	442

Table 2 continued

Log unit	Results of V-FWS method				Results of V-Fala method						
					Averaging in depth section of meters:						
	Av	Min	Max	S.D.	30	20	12	10	8	2.5	M
Upper Permian, Zechstein, Younger Halite Na3 (2993.5-3118.9 m), N = 1255											
RHOB	2.06	1.98	2.87	0.11							
GR	10	5	106	11							
DTP [μs/m]	228	199	325	11	220	223	225	225	225	227	224
DTS [μs/m]	408	339	448	10	393	388	388	386	384	354	382
Upper Permian, Zechstein, Main Anhydrite A3 (3119-3151.4 m), N = 325											
RHOB	2.92	2.61	2.97	0.03							
GR	6	5	10	1							
DTP [μs/m]	173	170	205	4	203	194	186	184	181	172	187
DTS [μs/m]	323	315	393	10							
Upper Permian, Zechstein, Grey Salt Clay I3 (3151.5-3157.4 m) N = 60											
RHOB	2.44	2.27	2.76	0.12							
GR	75	15	95	18							
DTP [μs/m]	289	183	362	48	231	234	238	242	252	285	247
DTS [μs/m]	406	385	428	14	425	438	469	462	445	398	440
Upper Permian, Zechstein, Screening Anhydrite A2G (3157.5-3158.9 m), N = 15											
RHOB	2.87	2.77	2.91	0.04							
GR	14	8	33	7							
DTP [μs/m]	187	173	223	15	224	224	220	218	215	206	218
DTS [μs/m]											
Upper Permian, Zechstein, Older Halite Na2 (3159-3319.9 m), N = 1610											
RHOB	2.05	1.98	2.68	0.04							
GR	13	4	176	25							
DTP [μs/m]	225	199	241	2	220	222	223	223	223	224	222
DTS [μs/m]	407	334	452	6	399	396	394	394	391	371	391
Upper Permian, Zechstein, Basal Anhydrite A2 (3320-3323.9 m), N = 40											
RHOB	2.87	2.2	2.94	0.16							
GR	9	5	26	4							
DTP [μs/m]	177	167	214	12	173	178	186	183	177	174	179
DTS [μs/m]	318	295	330	10							
Upper Permian, Zechstein, Main Dolomite Ca2 (3324-3333.4 m), N = 95											
RHOB	2.71	2.56	2.95	0.06							
GR	42	13	60	11							
DTP [μs/m]	190	164	234	21	170	172	186	179	183	187	179
DTS [μs/m]	331	294	393	29							
Upper Permian, Zechstein, Upper Anhydrite A1G (3333.5-3400.9 m), N = 675											
RHOB	2.91	2.77	2.97	0.03							
GR	10	4	43	7							
DTP [μs/m]	173	165	195	7	174	173	173	173	172	172	173
DTS [μs/m]	324	306	403	16							
Upper Permian, Zechstein, Oldest Halite Na1 (3401-3404.9 m), N = 40											
RHOB	2.4	2.08	2.89	0.33							
GR	5	4	5	0							
DTP [μs/m]	187	160	209	17	181	178	176	175	174	183	178
DTS [μs/m]	374	323	415	35							

Table 2 continued

Log unit	Results of V-FWS method				Results of V-Fala method						
					Averaging in depth section of meters:						
	Av	Min	Max	S.D.	30	20	12	10	8	2.5	M
Upper Permian, Zechstein, Lower Anhydrite A1D (3405-3539.4 m), N = 1345											
RHOB	2.92	2.69	3.01	0.03							
GR	7	2	20	3							
DTP [μs/m]	172	160	215	10	176	173	172	171	171	171	172
DTS [μs/m]	318	286	392	19	416	378	348	333	322	297	349
Upper Permian, Zechstein, Zechstein Limestone Ca1 (3539.5-3540.2 m), N = 8											
RHOB	2.8	2.79	2.83	0.01							
GR	46	27	57	10							
DTP [μs/m]	156	154	160	2	235	222	209	199	185	156	201
DTS [μs/m]	289	277	299	8							
Lower Permian, Rotliegend P1 (3540.3-3623.5 m), N = 1108											
RHOB	2.41	2.21	2.8	0.08							
GR	42	26	62	7							
DTP [μs/m]	245	155	308	20	247	247	246	246	246	244	246
DTS [μs/m]	421	272	484	40	525	495	477	469	445	330	457

Symbols: Av – average value, Min – minimum value, Max – maximum value, S.D. – standard deviation value, M – mean value of DTP slowness and DTS slowness for each stratigraphic unit, RHOB – bulk density [g/cm^3], GR – gamma ray [API], DTP – P-wave slowness, DTS – S-wave slowness

rocks, encountered in the profile. These data were treated as outliers and not used in subsequent processing.

The analysis of averaging results plotted *versus* depth (Fig. 9) unambiguously shows that information was lost in the course of the 20 m and 30 m averaging. It is clearly visible that all boundaries between the different stratigraphic units cannot be properly determined. To keep the slowness information of relatively thin beds at a realistic level, filtering should be stopped at the level of 12 m. More details can be seen on the selected section of the P1 stratigraphic unit (Fig. 10). The conclusions were similar to those obtained from the analysis of Figure 9.

To explore further aspects of filtering applied, additional plots (Fig. 11) were prepared for the selected sections of geological profile of the SW5 well: Middle Triassic, Tm3, 1989 m – Lower Triassic, Tp1, 2580 m (Table 3). Triassic formations in this section were differentiated enough to show the influence of lithology on the results of averaging.

The analysis of plots in Figure 11 was the basis for the similar conclusions which were derived from Figures 9 and 10 and Table 2. The primary data (2.5 m depth step) provided too much detailed information which cannot be directly used for seismic interpretation. Averaging at the level of a 30 m depth window resulted in the loss of some layers, distinctly differing in slowness from those in their immediate vicinity. In such cases, a better approach would be calculating a weighted average of slowness, using the thickness of selected layers which significantly differed in DT as a weight.

Taking in consideration all of the conclusions from filtering, a mean value of DTP slowness and DTS slowness for each stratigraphic unit selected in SW5 well was calculated (Table 2, value M). This mean M was also the basis for constructing the velocity models (Fig. 12). In Figure 12, the values for the slowness characteristic of stratigraphic units were plotted to illustrate the variability of this parameter. P-wave slowness correctness was successfully verified on the basis of the high correlation between DTP FWS (the V-FWS method) and DTP Fala (the V-Fala method).

Table 3

Stratigraphy and lithology of formations from middle part of SW5 well

Chrono-stratigraphic subdivision	Symbol	Depth of top [m]	Depth of bottom [m]	Lithology
Middle Triassic	Tm3	1989.5	2031	Upper Muschelkalk: limestones, marlstones, siltstones, mudstones, sandstones
	Tm2	2031	2079	Middle Muschelkalk: limestones, marlstones
	Tm1	2079	2256.5	Lower Muschelkalk: limestones, marlstones, mudstones, shales
Lower Triassic	Tp3	2256.5	2365.5	Upper Bunter Sandstone (Röt Formation): calcareous mudstones, limestones, marlstones, anhydrites
	Tp2	2365.5	2580	Middle Bunter Sandstone: red and brown mudstones, marlstones, limestones, anhydrites
	Tp1	2580	2919	Lower Bunter Sandstone: mudstones, brown calcareous siltstones, sandstones, limestones

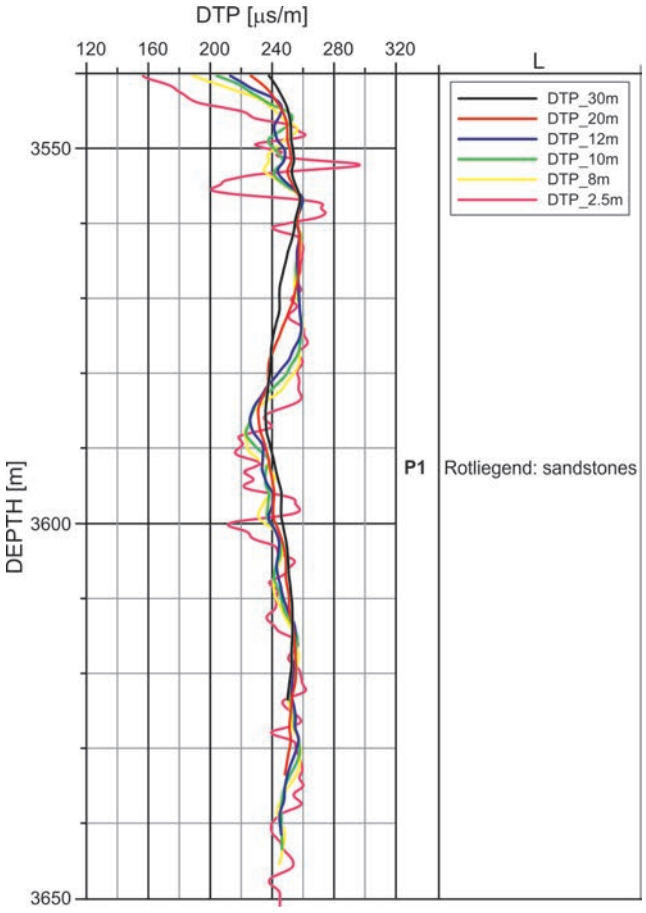

Fig. 10. Variability of averaged P-wave slowness, DTP, from V-Fala method, at depths of 3545–3648 m (P1, Rotliegend sandstones). Symbols: L – lithology, P1 – Lower Permian, DTP_30m – DTP after 30 m averaging, DTP_20m – DTP after 20 m averaging, DTP_12m – DTP after 12 m averaging, DTP_10m – DTP after 10 m averaging, DTP_8m – DTP after 8 m averaging, DTP_2.5m – DTP after 2.5 m averaging

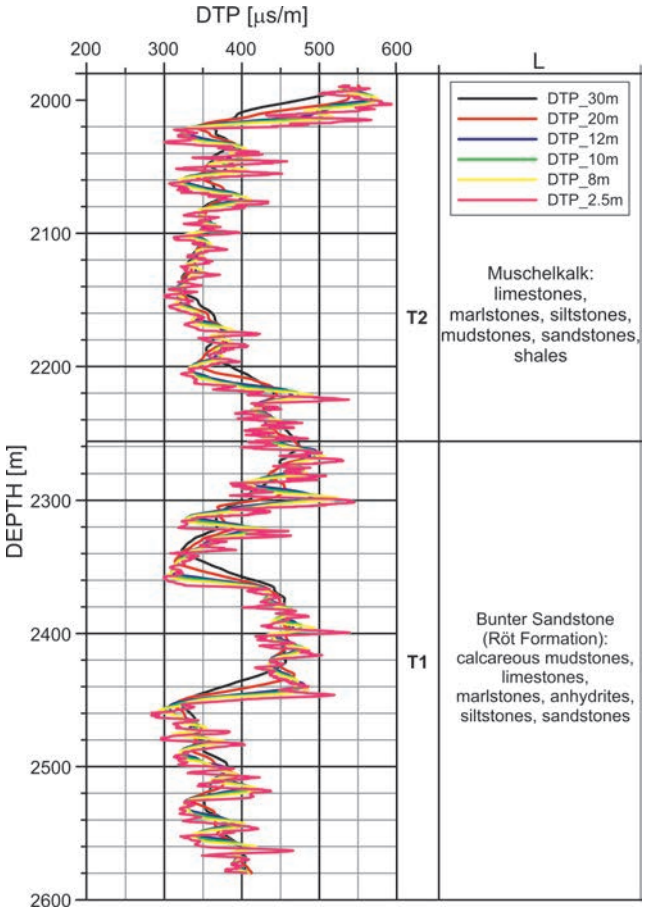

Fig. 11. Comparison of averaged S-wave slowness, DTS, from V-Fala method at depths of 1989 – 2920 m in SW5 well. Symbols: L – lithology, T2 – Middle Triassic, T1 – Lower Triassic, DTS_30m – DTS after 30 m averaging, DTS_20m – DTS after 20 m averaging, DTS_12m – DTS after 12 m averaging, DTS_10m – DTS after 10 m averaging, DTS_8m – DTS after 8 m averaging, DTS_2.5m – DTS after 2.5 m averaging

FREQUENCY INFLUENCE ON THE VELOCITY OF ELASTIC WAVES IN ACOUSTIC LOGS AND SEISMICS

The assumption that the velocity of body waves (P and S) in the frequency range of elastic waves used in applied geophysics (seismic and acoustic log) was not dispersive in many cases caused errors in velocity determinations. Considering the Aki and Richards equation (1980), employing a quality factor Q in the relationship between velocity of acoustic wave and velocity of seismic wave, the difference between two velocities could be analysed. The Aki and Richards equation (1980) was used in the following form:

$$\text{VPseis} \quad \text{VPacous} / \text{factor}$$

$$\text{factor} \quad 1 \quad \frac{1}{Q} \ln \frac{\text{Facous}}{\text{Fseis}} \qquad (2)$$

where: VPacous and VPseis were the velocities of the P – acoustic wave and P – seismic wave, respectively, Facous and Fseis were the frequencies of the P – acoustic wave and the P – seismic wave, respectively, and Q was a quality factor, related to the attenuation of elastic waves.

Several values of the factor were calculated to recognise the mutual influence of frequency and Q on velocity (Table 4).

Q values, related to lithology and stratigraphy, were chosen on the basis of the interpretation results for individual acoustic full waveforms in several wells from the study area (Górecki *et al.*, 2010; Jarzyna *et al.*, 2011a). The interpretation of amplitude spectra of individual waveforms in FalaFWS was the basis of Q values determination (Cheng, 1989). For the factor calculations, minimal (Q = 7 for claystones) and mean (Q = 15–45 for sandstones and limestones) and maximal Q values (Q = 90 related to rock salt) were used (Table 4). The factor was constant for selected parameters (frequencies and Q), so it was used to illustrate the changes in velocity. In the lower part of Table 4, two examples of P-wave velocity, 3000 m/s and 4500 m/s, are

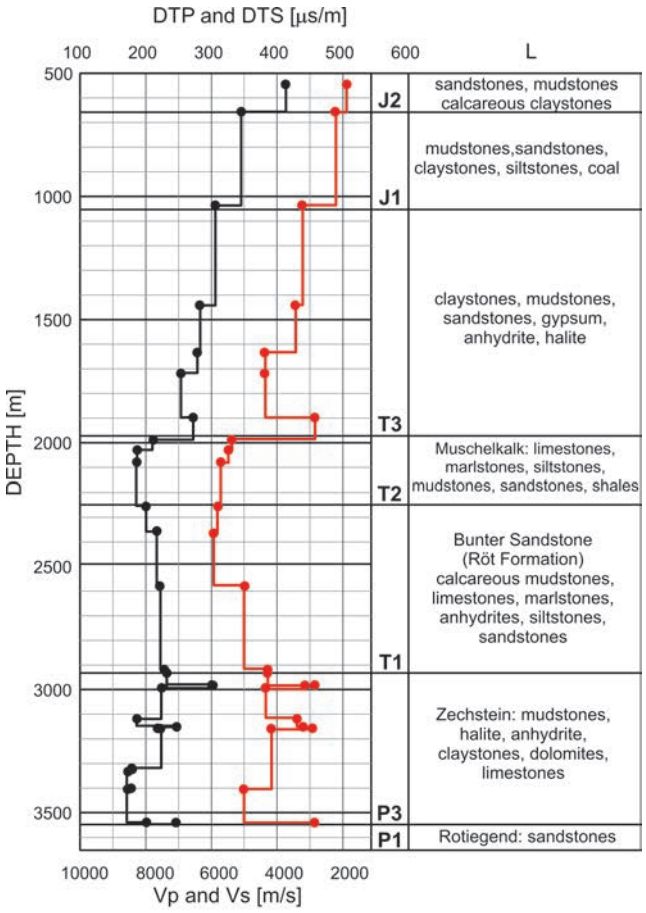

Fig. 12. Illustration of variability of mean values of P-wave slowness, DTP, and mean S-wave slowness, DTS, in selected lithostratigraphic units in SW5 well. Symbols: L – lithology, J2 – Middle Jurassic, J1 – Lower Jurassic, T3 – Upper Triassic, T2 – Middle Triassic, T1 – Lower Triassic, P3 – Upper Permian, P1 – Lower Permian

shown. They were determined from an acoustic log and selected as typical for many layers in the geological profile of the SW5 well. The respective values of the seismic P-wave velocities, according to factors depending on assumed frequencies and Q, were included to compare the change in velocity, due to different frequency of acoustic wave and seismic wave and the attenuation ability of rock. The analysis of values from Table 4 suggests that the combination of wave frequency and quality factor, rather than individual parameters, determine the degree of seismic wave velocity reduction by comparison with acoustic wave velocity.

CONCLUSIONS

Sonic log measurements (V-FWS method) provide slowness values directly from a borehole. However, in a number of depth intervals, records of S-wave slowness cannot be obtained. These depth intervals are associated with rock formations with poor elastic properties, fractured, and with high clay content. In such sections, the missing results can be supplemented with data interpreted from the acoustic waveforms, using the V-Fala method. Both methods provide results only for the intervals, where full waveform data are recorded. Thus, the data are influenced by the recording conditions, such as variable well diameter, changes in borehole fluid parameters with depth, or a distorted configuration of the sonic tool.

The V-EST method provides slowness data for all depth intervals, where a comprehensive interpretation for lithology and porosity is carried out. Usually, these sections of wells are longer than those, where the recorded acoustic full waveforms are available. In order to perform calculations using the V-EST method, the elastic parameters of matrix components and the parameters related to the pore fluids have to be set. The accuracy of the adopted parameters determines the accuracy of the V-EST method results.

The results of the V-Fala method are dependent on the vertical distance between recording points and the vertical sampling interval, adopted for the interpretation. Similarly, the vertical sampling interval, applied in the calculations for the V-EST method, affect the results.

Filtering (averaging) of results can be done using a running average on raw data from measurements (V-FWS method) and on the results of the V-Fala method. Depth windows for filtering should be carefully selected according to the expected vertical resolution of seismic, as well as stratigraphic and lithological data. A depth window for averaging that is too wide can lead to a loss of information. When thin beds with different velocities are to be included in a velocity model, the calculation of a weighted average is recommended.

The consistency of the P-wave slowness obtained from applications of all three methods is high, so that the P-wave data could be used interchangeably in seismic interpretations. A similar conclusion is true for S-wave slowness, al-

Table 4

Relationships between various parameters influencing velocity

Facous [kHz]	20	20	12	12	10	10	10	6
Fseis [Hz]	40	40	40	40	60	60	60	60
Q	16	45	45	16	10	7	90	45
Factor	1.1237	1.0440	1.0404	1.1135	1.1629	1.2328	1.0181	1.0326
VPseis [m/s] for VPacous = 3000 m/s	2670	2874	2884	2694	2580	2433	2947	2905
VPseis [m/s] for VPacous = 4500 m/s	4005	4310	4327	4041	3870	3650	4420	4358

though the scatter of results is considerable. Several outliers can be adjusted during the analysis of results, through the removal of unrealistic or unclear recordings of acoustic full waveforms.

Acknowledgements

The study was completed as a part of the project "Improvement of the effectiveness of seismic survey for prospection and exploration for natural gas deposits in Rotliegend formations, MNiSW WND. POIG.01.01.02.00.122/09". The authors would like to thank Wojciech Górecki for the invitation to take part in the project. They would also like to express their gratitude to the Zielona Góra branch of PGNiG S.A. and the company Geofizyka Toruń S.A. for making the survey data available to them. The authors would like to thank the Reviewers and Editors for their work which resulted in improving of the paper.

REFERENCES

Aki, K., Richards, P. G., 1980. *Quantitative Seismology*, Volume 1. W. H. Freeman and Co., 573 pp.

Bała, M., 1994. Effect of water and gas saturation in layers on elastic parameters of rocks and reflection coefficients of waves. *Acta Geophysica Polonica*, 42: 149–158.

Bała, M. & Cichy, A., 2003. Calculation of longitudinal and shear waves velocities based on theoretical models and well logging data. *Przegląd Geologiczny*, 51: 1058–1063. [in Polish, English asbtract].

Bała, M. & Cichy, A., 2006. *Methods of Calculating P and S Waves Velocities as a Function Based on Theoretical Models and Well Logging Data – Program ESTYMACJA*. AGH University of Science and Technology Press, Kraków, 89 p. [In Polish].

Bała, M. & Cichy, A., 2007. Comparison of P-wave and S-wave velocities estimated from Biot-Gassmann and Kuster-Toksöz models with results obtained from acoustic wavetrains interpretation. *Acta Geophysica Polonica*, 55: 222–230.

Biot, M. A., 1956. Theory of propagation of elastic waves in a fluid saturated porous solid. Low frequency range. *Journal of the Acoustical Society of America,* 28: 168–191.

Boyer, S. & Mari, J. L., 1997. *Seismic Surveying and Well Logging*. Editions Technip. Paris, 192 pp.

Cheng, C. H., 1989. Full waveform inversion of P-waves for Vs and Qp. *Journal of Geophysical Research*, 94: 15619–15625.

Dadlez, R., Marek, S. & Pokorski, J., 2000. *Geological Map of Poland without Cenozoic Deposits (1:1 000 000)*. Polish Geological Institute, Warsaw.

Gassmann, F., 1951. Über die Elastizitat poroser Medien. *Vierteljahrsschrift der Naturforschenden Gesellschaft*, 96: 1–23. Zurich.

Górecki, W., Jarzyna, J., Bała, M., Czopek, B., Krakowska, P., Nowak, J. & Wawrzyniak-Guz, K., 2010. *Improvement of the Effectiveness of Seismic Survey for Prospection and Exploration for Natural Gas Deposits in Rotliegend Formations*. *Project Report, III Stage, November 2010*. Research program: MNiSW WND. POIG.01.01.02.00.122/09. Archive of Fossil Fuels Department, FGGEP AGH, Krakow [In Polish].

Halliburton Logging Services, 1991. *Log Interpretation Charts.* Appendix, APP-4a, APP-4b

Jarzyna, J., Bała, M., Cichy, A., Gądek, W., Gąsior, I., Karczewski, J., Marzencki, K., Stadtmuller, M., Twaróg, W. & Zorski, T., 2002. *Processing and Interpretation of Well-logging Data by Means of the GeoWin System*. Arbor, Kraków, 136 pp. [In Polish].

Jarzyna, J., Bała, M., Cichy, A., Gądek, W., Karczewski, J., Marzencki, K., Stadtmuller, M., Twaróg, W., Zorski, T., Jarzyna, J., Bała, M. & Cichy, A., 2007. *Processing and Interpretation of Well-logging Data by Means of the GeoWin System*. *Pt. 2, New Applications And supplements*. Arbor, Kraków, 86 pp. [In Polish].

Jarzyna, J., Bała, M., & Cichy, A., 2010. Elastic parameters of rocks from well logging in near surface sediments. *Acta Geophysica*, 58: 34–48.

Jarzyna, J., Bała, M., Krakowska, P. & Wawrzyniak-Guz K., 2011a. Scaling of the well logging data for the velocity models in seismics. *Kwartalnik AGH, Geologia*, 37: 401–446. [In Polish].

Jarzyna, J., Bała, M. & Krakowska, P., 2011b. Velocity models for seismics based on well log data. *Kwartalnik AGH, Geologia*, 37: 447–473. [In Polish].

Kimball, C. & Marzetta, T. L., 1984. Semblance processing of borehole acoustic array data. *Geophysics*, 49: 274–281.

Marzec, P., Niepsuj, M., Słonka, Ł. & Pietsch, K., 2013. Application of 2-D forward seismic modelling for improved imaging of sub-salt Rotliegend strata in Polish Basin. *Annales Societatis Geologorum Poloniae*, 83: 65–80.

Pharaoh, T. C., Dusar, M., Geluk, M. C., Kockel, F., Krawczyk, C. M., Krzywiec, P., Scheck-Wenderoth, M., Thybo, H., Vejbæk, O. V. & van Wees, J. D., 2010. Tectonic evolution. In: Doornenbal, J. C. & Stevenson, A. G. (eds), *Petroleum Geological Atlas of the Southern Permian Basin Area*. EAGE Publications b.v., Houten, pp. 25–57.

Pietsch, K., Marzec, P., Niepsuj, M. & Krzywiec, P., 2012. The influence of seismic velocity distribution on the depth imaging of the sub-Zechstein horizons in areas affected by salt tectonics: a case study of NW Poland. *Annales Societatis Geologorum Poloniae*, 82: 263–277.

Theys, P., 1999. *Log Data Acquisition and Quality Control, the Second Edition*. Editions Technip, Paris, 453 pp.

Wagner, R., 1998. Cechsztyn. In: Dadlez, R., Marek, S. & Pokorski, J. (eds), *Atlas paleogeograficzny epikontynentalnego permu i mezozoiku w Polsce (1 : 2 500 000)*. Polish Geological Institute, Warsaw. [In Polish].

Ziegler, P. A., 1990. *Geological Atlas of Western and Central Europe, 2nd Edition*. Shell Internationale Petroleum Maatschappij B.V. and Geological Society Publishing House, Bath, 239 pp.